

Synthesis, characterization, and Pb²⁺ ion sensing application of hexa-armed dansyl end-capped poly(ϵ -caprolactone) star polymer with phosphazene core

Mesut Gorur,¹ Erdinc Doganci,² Faruk Yilmaz,³ Umit Isci³

¹Department of Chemistry, Istanbul Medeniyet University, 34700 Istanbul, Turkey

²Department of Science Education, Kocaeli University, 41380 Kocaeli, Turkey

³Department of Chemistry, Gebze Technical University, 41400 Kocaeli, Turkey

Correspondence to: M. Gorur (E-mail: mesut.gorur@medeniyet.edu.tr) and U. Isci (E-mail: u.isci@gtu.edu.tr)

ABSTRACT: Novel hexa-armed dansyl end-capped poly(ϵ -caprolactone) (PCL) star polymer with phosphazene core (**P2**) was prepared via ring opening polymerization (ROP) and esterification reactions. **P2** showed dual fluorescence emission when excited at 328 nm in acetonitrile : water (6 : 4) due to twisted intramolecular charge transfer (TICT) between dimethylamino and naphthalene units in the dansyl moiety. TICT emission band (A band) in the emission spectra red-shifted with increasing solvent polarity. **P2** responded to the addition of Pb²⁺, Hg²⁺, Co²⁺, Cd²⁺, Mn²⁺, and Zn²⁺ metal ions by decreasing TICT emission band with slight bathochromic shifts. The highest quenching efficiency was observed for Pb²⁺ ion with Stern–Volmer constant of 324.74M⁻¹. The Stern–Volmer plot for Pb²⁺ was rather linear with the increasing concentration of the quencher, indicating a dynamic (collisional) quenching mechanism. Stern–Volmer constants for Hg²⁺, Co²⁺, Cd²⁺, Mn²⁺, and Zn²⁺ ions were found to be 212.33, 189.21, 36.24, 20.84, and 20.69, respectively. Besides, the highest quenching efficiency (94.24%) was attained in the presence of Pb²⁺, suggesting that **P2** could be employed as a potential Pb²⁺ chemical probe. © 2015 Wiley Periodicals, Inc. *J. Appl. Polym. Sci.* **2015**, *132*, 42380.

KEYWORDS: functionalization of polymers; optical properties; polyesters; ring-opening polymerization; sensors and actuators

Received 11 March 2015; accepted 19 April 2015

DOI: 10.1002/app.42380

INTRODUCTION

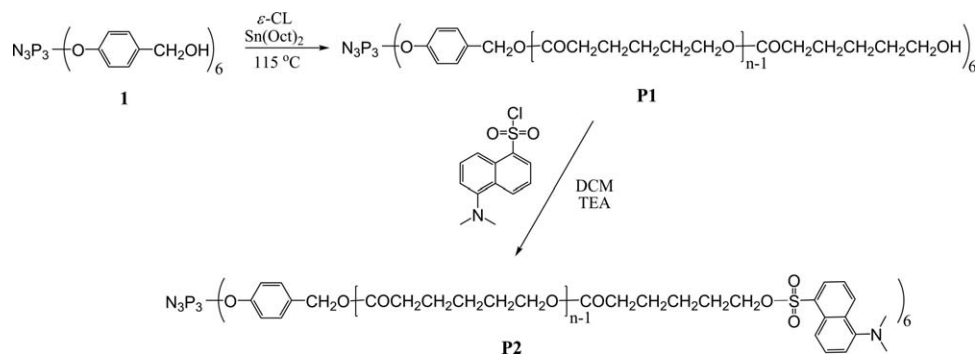
Qualitative and quantitative monitoring of heavy metal ions in the environment (water or soil) has attracted a great deal of attention due to health and safety considerations. While some of them are highly toxic for human health, such as lead and mercury, some others are among the essential micronutrients for animals and plants.^{1–4} The accumulation of the heavy metals in the ecosystem majorly occurs via industrial processes.^{5,6} The use of old water pipes, lead-based old paints, and ceramic glazes are among the other sources of Pb²⁺ ion in the environment.⁷ Accumulation of lead in the human body can cause damage to brain and kidney tissues, retardation of mental, behavioral and physical development, and other health problems.^{5,8,9} According to the report of World Health Organization (WHO), Pb²⁺ ion concentration in drinking water must not exceed 10 $\mu\text{g L}^{-1}$. Hg²⁺ is another most prevalent and toxic heavy metal ion whose accumulation in the environment occurs via oceanic and volcanic emissions, gold mining, solid waste incineration, combustion of fossil fuels, and industrial processes.^{10,11} Hg²⁺ ions

in the environment can be transformed into lipophilic organo-mercury derivatives (CH₃HgX) and accumulates in the human body through the food chain.¹² It severely damages the central nervous and endocrine systems, as well as it causes digestive and cardiac problems.^{1,13,14}

The development of sensitive, robust, reliable, and portable analysis methods for the detection of metal ions has drawn a great deal of attention. In this respect, fluorescence spectroscopic method has significant advantages regarding sensitivity, selectivity, and response time.^{15,16} Considerable scientific efforts have been invested in the development of fluorescent chemosensors toward a variety of biological materials, cations, and anions.^{13,15,17–23} Dansyl fluorophore, which consists of dimethylamino moiety as a donor part and naphthalene sulfonyl as an acceptor part, has been widely used in fluorescence sensing applications due to its strong fluorescence in the visible region with high quantum yields.^{24,25} Besides, fluorescence emission spectrum of dansyl fluorophore is very sensitive to polarity and pH changes in the analytic media.^{26,27} Zhao and Zhong

Additional Supporting Information may be found in the online version of this article.

© 2015 Wiley Periodicals, Inc.



Scheme 1. Synthetic procedure for the preparation of dansyl end-capped PCL star polymer with phosphazene core (P2).

synthesized dansyl-functional cholate foldamers for the selective fluorescence detection of Hg^{2+} ions.²⁸ Chen and coworkers prepared dansyl-functional peptidocalix[4]arene fluorescence chemosensor for the selective detection of fluoride ions.²⁹ He and coworkers reported that dansyl-functional aminoquinoline derivative can be employed in ratiometric detection of Zn(II) cation.³⁰ Liu and coworkers prepared dansyl-labeled poly(*N*-isopropylacrylamide) microgels to be used as fluorescent Cu^{2+} sensor and showed that thermo-induced collapse of the sensing material remarkably increased its detection sensitivity.³¹

Star-shaped polymers having multiple arms joined at the central core have attracted the attention of scientists due to their unique shape and possible processing advantages resulting from their compact structure.^{32,33} They have less entanglement in the solid state, high solubility in various organic solvents, as well as lower solution and bulk viscosities compared to linear ones having similar molecular weights.³⁴ Phosphonitric trimer derivatives having proper functional groups have been employed as the connecting (core) unit for the preparation of star-shaped polymers via core-first (divergent)^{35,36} and arm-first (convergent) approaches.³⁷ Besides, well-defined miktoarm star-shaped polymers have been prepared using multifunctional core compounds having different polymerization initiating and click coupling sites.^{38,39}

In this study, we are reporting synthesis, characterization, and metal ion sensing application of novel hexa-armed dansyl end-capped poly(ϵ -caprolactone) star polymer with phosphazene core (P2) (Scheme 1). To the best of our knowledge, this is the first report on the synthesis and metal ion sensing application of dansyl-functional star polymer with phosphazene core. P2 was prepared in a two-step synthetic procedure including ring opening polymerization (ROP) of ϵ -caprolactone (ϵ -CL) and esterification reactions. Chemical structures of the obtained polymers (P1–P2) were confirmed by FTIR and 1H -NMR spectroscopic techniques. Then, the fluorescence responses of P2 in the presence of Pb^{2+} , Hg^{2+} , Co^{2+} , Cd^{2+} , Mn^{2+} , and Zn^{2+} metal ions in the analytic media were investigated by fluorescence spectrophotometric method.

EXPERIMENTAL

Materials

ϵ -CL (Aldrich, 97%) was dried over calcium hydride, distilled under reduced pressure ($97^\circ C$, 10 mmHg) and stored over dry 4-Å molecular sieves. Tetrahydrofuran (THF, Aldrich, 99%) was dried

by refluxing over violet sodium benzophenone ketyl and distilled under dry argon atmosphere. Methanol (Merck, 99%) was dried over activated 4-Å molecular sieves and freshly distilled before using. Hexachlorocyclotriphosphazene (Aldrich, 99%), sodium hydride (60% in mineral oil, Merck), 4-hydroxybenzaldehyde (98%, Alfa Aesar), tetraethylammonium bromide (99%, Aldrich), sodium borohydride ($NaBH_4$, 98%, Alfa Aesar), tin(II) 2-ethylhexanoate ($Sn(Oct)_2$, 95%, Aldrich), dansyl chloride (Aldrich, 99%), triethylamine (TEA, Aldrich, 99.5%), methylene chloride (DCM, Aldrich, 99.5%), cadmium chloride (Aldrich, 99.0%), lead(II) nitrate (Aldrich, 99%), cobalt(II) chloride hexahydrate (Aldrich, 99%), manganese(II) chloride (Aldrich, 99%), zinc chloride (Aldrich, 98%), mercury(II) chloride (Aldrich, 99.5%), and triethylamine (TEA, $\geq 99.5\%$) were used as received.

Instrumentation

1H - and ^{31}P -NMR spectra were measured on a Varian UNITY INOVA 500 MHz (202 MHz for ^{31}P) spectrometer in $CDCl_3$ and d_6 -DMSO solutions at $25^\circ C$. H_3PO_4 (85%) was employed as the external reference for ^{31}P NMR measurements. Attenuated total reflectance Fourier transform infrared spectroscopy (ATR-FTIR) spectra were obtained on Perkin-Elmer Spectrum Two™ spectrometer equipped with Perkin Elmer UATR Two diamond ATR accessory and the results were uncorrected. Average molecular weights and molecular weight distributions of the star polymers were estimated on an Agilent 1260 Infinity GPC/SEC Instruments consisting of a pump, a refractive index detector, and two columns (Agilent PLgel 5 μm MIXED-C, 7.5×300 mm) which was calibrated using linear polystyrene standards. THF was employed as the eluent at a flow rate of 1 mL/min at $40^\circ C$. Melting points (T_m) and crystallization temperatures (T_c) of the star polymers were determined on Perkin Elmer differential scanning calorimeter (DSC) 8500 double-furnace differential scanning calorimeter under nitrogen flow (20 mL/min) at a heating rate of $10^\circ C/min$. Thermogravimetric analysis (TGA) was performed on a Perkin Elmer STA 6000 simultaneous thermal analyzer with a heating rate of $10^\circ C/min$ from room temperature up to $700^\circ C$ under nitrogen atmosphere. UV-vis and fluorescence spectra were measured using quartz cuvettes (1-cm path length) on Shimadzu UV-2600 and Agilent Cary Eclipse spectrophotometers, respectively.

Synthesis of $N_3P_3-(OC_6H_4-p-CH_2OH)_6$ (1)

$N_3P_3-(OC_6H_4-p-CH_2OH)_6$ was synthesized using the method reported in the literature.³²

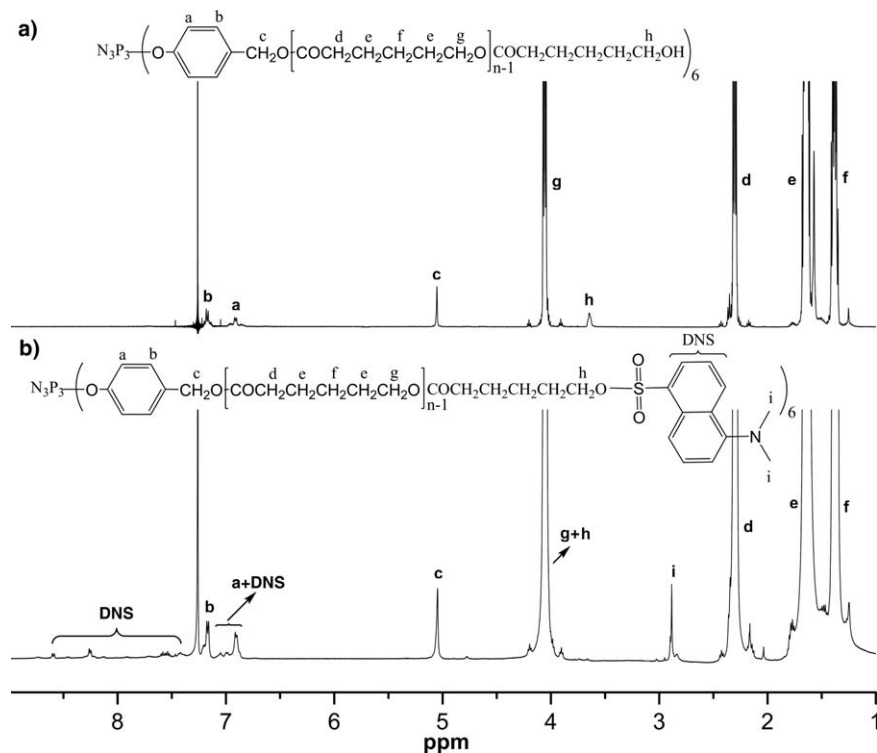


Figure 1. $^1\text{H-NMR}$ spectra of (a) **P1** and (b) **P2** in CDCl_3 at room temperature.

Yield: 87%. m.p.: 218–219°C. $m/z = 874.37$ $[\text{M}+1]^+$. FTIR (cm^{-1}): 3350 (OH, strong, broad); 2905 and 2878 (C–H); 1162 (P=N–); 955 (P–O–Ph); 1606 (C–C_{Ph}). $^1\text{H-NMR}$ (DMSO- d_6 , δ , ppm): 4.47 (d, CH_2 , 12H); 5.24 (t, OH, 6H); 7.20, 7.19 and 6.81, 6.80 (AA'BB' pattern, C_6H_4 , 24H). $^{31}\text{P-NMR}$ (^1H decoupled, DMSO- d_6 , δ , ppm): 9.93 (s).

Synthesis of Hexa-Armed PCL Star Polymer with OH Functional End Units ($\text{N}_3\text{P}_3\text{-(PCL-OH)}_6$) (**P1**)

$\text{N}_3\text{P}_3\text{-(PCL-OH)}_6$ (**P1**) was synthesized according to the method reported in the literature.³²

Tin(II) 2-ethylhexanoate ($\text{Sn}(\text{Oct})_2$) (0.0487 g, 0.120 mmol) and $\text{N}_3\text{P}_3\text{-(OC}_6\text{H}_4\text{-}p\text{-CH}_2\text{OH)}_6$ (**1**) (0.1 g, 0.114 mmol) was added to a fire dried polymerization tube. Then, $\epsilon\text{-CL}$ (2.743 g, 24.035 mmol) was added and the mixture was stirred under argon atmosphere until a clear solution was obtained. After the reaction tube was tightly closed, it was immersed in a thermostated oil bath at 115°C and stirred for 24 h. Then, the mixture was cooled to room temperature, the raw product was dissolved in methylene chloride (3 mL) and purified by precipitating in cold methanol. **P1** was collected by filtering through a glass filter (G4) and dried under reduced pressure at ambient temperature until a constant weight.

Yield: 2.607 g (91.4%). $M_{n,\text{NMR}}$: 22,789 g/mol; $M_{n,\text{GPC}}$: 18,700 g/mol; M_w/M_n : 1.30. FTIR (cm^{-1}): 3355 (O–H, weak, broad); 2944 (C–H), 2866 (C–H); 1722 (C=O); 1470 (C–H); 1240 ((C=O)–O); 1168 (P=N); 1046 (C–O–C); 958 (P–O–Ph); 732 (P–N). $^1\text{H-NMR}$ (CDCl_3 , δ , ppm): 7.18, 7.16 and 6.92, 6.90 (AA BB pattern, C_6H_4 in phosphazene core);

5.05 (s, $\text{C}_6\text{H}_4\text{CH}_2\text{O}$); 4.06 (m, $\text{CH}_2\text{OC}(\text{O})$ in PCL); 3.65 (t, terminal CH_2OH in PCL); 2.30 (m, $\text{OC}(\text{O})\text{CH}_2$ in PCL), 1.65 (m, $\text{C}(\text{O})\text{CH}_2\text{CH}_2\text{CH}_2\text{CH}_2\text{CH}_2\text{OC}(\text{O})$ in PCL), 1.38 (m, $\text{C}(\text{O})\text{CH}_2\text{CH}_2\text{CH}_2\text{CH}_2\text{CH}_2\text{OC}(\text{O})$ in PCL).

Synthesis of Hexa-Armed PCL Star Polymer with Dansyl Functional End Units ($\text{N}_3\text{P}_3\text{-(PCL-Dansyl)}_6$) (**P2**)

P1 ($M_{n,\text{NMR}} = 22,789$ g/mol, 0.5 g, 0.0219 mmol) was dissolved in anhydrous DCM (10 mL) under an oxygen-free argon atmosphere. After TEA (0.027 g, 0.263 mmol) was added, the solution was cooled to -10°C using an ice–salt mixture and dansyl chloride (0.053 g, 0.197 mmol) in anhydrous DCM (10 mL) was added dropwise to the reaction mixture within 20 min. Then, the cooling ice–salt bath was removed and the reaction mixture was continued stirring for 48 h at room temperature. The solution was concentrated to about 5 mL by rotary evaporation and dansyl functional polymer (**P2**) was purified by precipitating in cold methanol. **P2** was collected by filtering through a glass filter (G4) and dried under reduced pressure at ambient temperature until a constant weight.

Yield: 0.457 g (86.2%). $M_{n,\text{NMR}}$: 24,188 g/mol; $M_{n,\text{GPC}}$: 19,800 g/mol; M_w/M_n : 1.29. FTIR (cm^{-1}): 2946 (C–H), 2866 (C–H); 1722 (C=O); 1471 (C–H); 1240 ((C=O)–O); 1176 (P=N); 1046 (C–O–C); 960 (P–O–Ph); 732 (P–N). $^1\text{H-NMR}$ (CDCl_3 , δ , ppm): 8.60, 8.25, 7.56, 7.43, and 7.00 (CH, in dansyl moiety); 7.18, 7.16 and 6.92, 6.90 (AABB pattern, C_6H_4 in phosphazene core); 5.05 (s, $\text{C}_6\text{H}_4\text{CH}_2\text{O}$); 4.05 (m, $\text{CH}_2\text{OC}(\text{O})$ in PCL a); 2.88 (s, $-\text{N}(\text{CH}_3)_2$, in dansyl moiety); 2.30 (m, $\text{O}(\text{CO})\text{CH}_2$ in PCL), 1.64 (m, $\text{COCH}_2\text{CH}_2\text{CH}_2\text{CH}_2\text{CH}_2\text{O}(\text{CO})$ in PCL), 1.38 (m, $\text{COCH}_2\text{CH}_2\text{CH}_2\text{CH}_2\text{CH}_2\text{O}(\text{CO})$ in PCL).

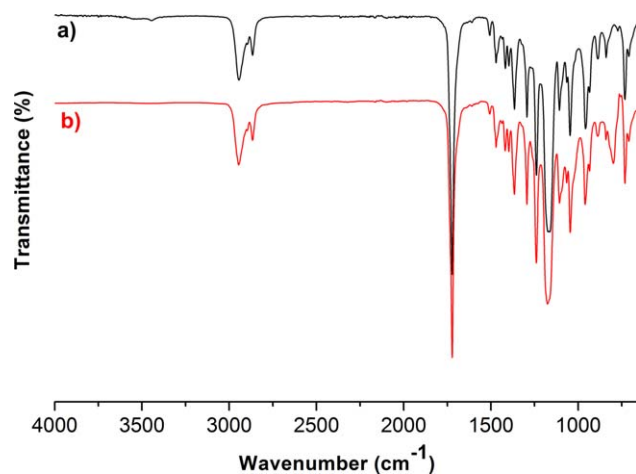


Figure 2. FTIR spectra of (a) **P1** and (b) **P2**. [Color figure can be viewed in the online issue, which is available at wileyonlinelibrary.com.]

Metal Ion Sensing Applications of Dansyl End-Capped PCL Star Polymer (**P2**) via Fluorescence Spectroscopy

Metal ion sensing applications of dansyl end-capped PCL star polymer with phosphazene core (**P2**) were performed via fluorescence spectroscopy. The general experimental procedure was as follows: Firstly, definite amounts of dansyl end-capped PCL star polymer (**P2**) was dissolved in ACN : water (6 : 4) solvent mixture at room temperature. Then, the fluorescent responses of **P2** upon the addition of prescribed amount of targeted metal ions were measured.

RESULTS AND DISCUSSION

The dansyl end-capped PCL star polymer with phosphazene core (**P2**) was prepared in a two-step synthetic procedure, including ROP and esterification reactions (Scheme 1). In the first step, the hydroxyl end-functional PCL polymer with phosphazene core (**P1**) was synthesized via ROP of ϵ -CL, initiated by hexa-hydroxyl functional phosphazene derivative (**1**) in the presence of tin 2-ethyl hexanoate ($\text{Sn}(\text{Oct})_2$) as the coordination–insertion catalyst. Then, dansyl functional groups were attached to the termini of the polymer arms of **P1** via esterification reaction between hydroxyl end-groups of **P1** and dansyl chloride, yielding **P2**.

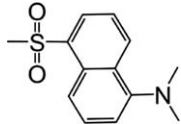
Chemical structures of the synthesized hydroxyl and dansyl end-functional polymers (**P1** and **P2**, respectively) were investigated via $^1\text{H-NMR}$ and FTIR spectroscopies. In the $^1\text{H-NMR}$

spectrum of **P1** [Figure 1(a)], methylene proton signals of ϵ -CL repeating units were observed at 4.06 (H_g), 2.30 (H_d), 1.65 (H_e), and 1.38 (H_f) ppm. The signal observed at 3.65 ppm was ascribed to terminal methylene protons (H_h) and it indicates that the polymer chains of **P1** star polymer was terminated by hydroxyl end units.⁴⁰ Besides, the protons of phosphazene core unit gave resonances at 5.05 (H_c), 6.90–6.92 (H_a), and 7.16–7.18 (H_b) ppm. The integration ratio between the terminal methylene protons (H_h) and the methylene protons next to the benzene ring (H_c) (H_h/H_c) was calculated as 1.01, while the theoretical value should be 1.00. The close proximity between these values indicated that the ROP of ϵ -CL was successfully initiated only by the hydroxyl functional groups of the phosphazene initiator (**1**). Upon esterification of **P1** with dansyl chloride, the signal of the terminal methylene protons (H_h) in the $^1\text{H-NMR}$ spectrum of **P1** [Figure 1(a)] moved to lower magnetic fields and overlapped by H_g methylene proton signals of the repeating units in the $^1\text{H-NMR}$ spectrum of **P2** [Figure 1(b)]. Besides, there appears new proton resonance signals and they were attributed to H_i methyl ($\delta = 2.88$ ppm) and aromatic CH protons ($\delta = 7.00, 7.43, 7.56, 8.25, \text{ and } 8.60$ ppm) in the terminal dansyl units.

FTIR spectral analysis of the synthesized star polymers (**P1** and **P2**) provides some complimentary information for their structural characterization. In the FTIR spectrum of **P1** and **P2** (Figure 2), the strong sharp peak observed at 1722 cm^{-1} was attributed to the carbonyl stretching frequency in the ϵ -CL repeating units of the polymer arms. The signals corresponding to symmetric and asymmetric CH stretching vibrations of the star polymers were observed around 2866 and 2944 cm^{-1} , respectively. Besides, CH bending band emerged around 1470 cm^{-1} . On the other hand, asymmetric and symmetric P=N–P stretching vibration bands in the phosphazene core appeared around 1168 and 732 cm^{-1} , respectively, while P–O–Ph stretching signals were observed around 958 cm^{-1} . These FTIR spectroscopic data confirm that **P1** and **P2** star polymers contain phosphazene moiety. Upon esterification reaction of **P1** with dansyl chloride, the weak and broad hydroxyl stretching band which was observed around 3555 cm^{-1} in the FTIR spectrum of **P1** [Figure 2(a)] clearly disappeared in that of **P2** [Figure 2(b)], indicating that the reaction was accomplished quantitatively.

The number- (M_n) and weight-average (M_w) molecular weights of the PCL star polymers with phosphazene cores (**P1** and **P2**) were estimated by gel-permeation chromatography (GPC). Their chromatograms were demonstrated in Supporting Information Figure SI-1 and SI-2 and the related data are summarized in

Table I. Molecular Weight Analysis of the Star Polymers with Different End-Functional Units

Polymers	$M_{n,\text{NMR}}^a$	$M_{n,\text{GPC}}^b$	$M_{w,\text{GPC}}^b$	M_w/M_n^b	End units
P1	22789	18300	25200	1.38	–OH
P2	24188	19800	26900	1.36	

^a $M_{n,\text{NMR}}$ was calculated using the data obtained from $^1\text{H-NMR}$ spectral analysis.

^b $M_{n,\text{GPC}}$, $M_{w,\text{GPC}}$, and M_w/M_n were obtained from GPC experiments based on linear polystyrene standards using THF as the eluent.

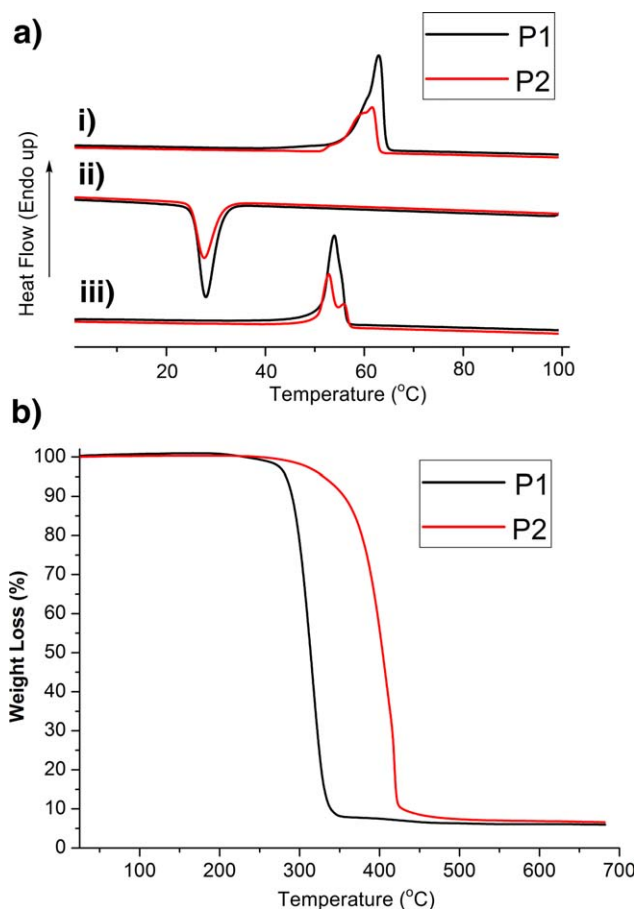


Figure 3. (a) DSC thermograms of **P1** and **P2** in the first heating (i), cooling (ii), and second heating run (iii); (b) TGA thermograms of **P1** and **P2**. [Color figure can be viewed in the online issue, which is available at wileyonlinelibrary.com.]

Table I. Both of the star polymers gave symmetrical unimodal elution peaks in these chromatograms and had low polydispersity values (PDI, M_w/M_n), indicating that the purified polymerization products contained only the desired star polymers. The number average molecular weights (M_n) of the star polymers could also be calculated from their $^1\text{H-NMR}$ spectra. The degree of polymerization (DP_n) for polymer arms of both star polymers was found as 32, which is equal to the integral area ratio between the signals of H_g methylene protons in PCL arms at 4.06 and that of H_h methylene protons at the termini of

polymer chains at 3.65 ppm (Figure 1). Thus, number-average molecular weights ($M_{n,\text{NMR}}$) were computed using the following formula: $M_{n,\text{NMR}} = \text{MW of the core unit} + 6 \times [32 (\text{DP}_n \text{ of the PCL arms}) \times 114.14 (\text{MW of } \epsilon\text{-CL repeating units})] + 6 \times \text{MW of chain end units}$. The inconsistency between $M_{n,\text{GPC}}$ and $M_{n,\text{NMR}}$ values attributed to differences between hydrodynamic volumes of the synthesized star polymers and the linear polystyrene standards which was used to calibrate GPC instrument. Therefore, the molecular weights of the star polymers calculated from $^1\text{H-NMR}$ spectral data are more dependable than those attained by conventional GPC analysis.

The melting and crystallization tendencies of hydroxyl (**P1**) and dansyl (**P2**) end-capped PCL star polymers, whose PCL arms are semi-crystalline in nature, were determined via DSC experiments. DSC thermograms of **P1** and **P2** [Figure 3(a)] demonstrates characteristic transitions for PCL polymers, such as melting and crystallization, in the first heating, cooling, and second heating runs. The DSC data summarized in Table II reveal that the attachment of dansyl end units via esterification reaction slightly reduced the onset melting temperature ($T_{m, \text{onset}}$). On the other hand, enthalpy of fusion (ΔH_m) and crystallinity (X_c) of **P2** were observed faintly higher than those of **P1**. It is thought that physical interactions between dansyl end units (such as π - π stacking) became influential to some extent on the regular rearrangement of semicrystalline PCL arms of **P2**.

Thermal stabilities of the star polymers (**P1** and **P2**) were measured via TGA experiments under nitrogen atmosphere at $10^\circ\text{C}/\text{min}$ heating rate from room temperature to 700°C . Percent weight loss/temperature curves of hydroxyl (**P1**) and dansyl (**P2**) end functional star polymers are depicted in Figure 3(b) and the data related to their onset ($T_{d, \text{onset}}$) and maximum ($T_{d, \text{max}}$) thermal decomposition temperatures as well as their percent char yields are summarized in Table II. In the literature, hydroxyl end-groups of PCL polymers were reported as thermally unstable and the concentration of hydroxyl end-groups were inversely proportional to $T_{d, \text{onset}}$ and $T_{d, \text{max}}$ values of the polymers.^{42,43} In the present study, incorporation of dansyl groups to the termini of PCL arms of the star polymers slightly increased $T_{d, \text{onset}}$ of the star polymers, however substantial enhancement was observed in their $T_{d, \text{max}}$ values. On the other hand, percent char yield of these polymers were found to be very close to each other.

The presence of dansyl groups in the star polymer (**P2**) was further supported by absorption and fluorescence spectroscopic investigations. The UV-vis spectrum of **P2** taken in acetonitrile

Table II. Thermal Properties of the Synthesized Star Polymers

Polymers	$T_{m2, \text{onset}}^a$	ΔH_{m2}^b	$X_{c2} (\%)^c$	$T_{d, \text{onset}} (^\circ\text{C})^d$	$T_{d, \text{max}} (^\circ\text{C})^e$	Char yield (%) ^f
P1	51.30	49.70	35.63	270.97	316.22	5.98
P2	50.60	55.60	39.86	303.15	418.78	6.58

^a $T_{m2, \text{onset}}$ is the onset melting points of the star polymers in the second heating runs.

^b ΔH_{m2} is the fusion enthalpies of the star polymers in the second heating runs.

^c X_{c2} is the crystallinity of the star polymers calculated using the equation $[X_{c2} = (\Delta H_{m2}/\Delta H_m^0) \times 100]$. ΔH_m^0 is the enthalpy of fusion for perfectly crystalline PCL and $\Delta H_m^0 = 139.5 \text{ J g}^{-1}$.⁴¹

^d $T_{d, \text{onset}}$ denotes the onset decomposition temperatures of the star polymers.

^e $T_{d, \text{max}}$ designates the temperature that corresponds to maximum rate of weight loss.

^f The percent of weight remained at 700°C .

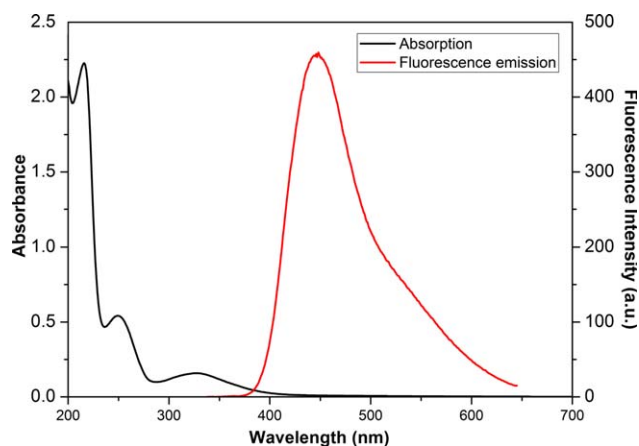


Figure 4. Absorbance and fluorescence emission spectra ($\lambda_{\text{ex}} = 328 \text{ nm}$) of **P2** ($1.34 \times 10^{-5} \text{ M}$) in ACN. [Color figure can be viewed in the online issue, which is available at wileyonlinelibrary.com.]

(ACN) (Figure 4) depicted a strong absorption at 215 nm, a shoulder peak at 250 nm, and a relatively weak absorption signal at 328 nm. The position of peak maxima and their relative intensities pose a rather good agreement with the literature.⁴⁴ The fluorescence emission spectrum of dansyl end-functional PCL star polymer (**P2**) in ACN is shown in Figure 4 ($\lambda_{\text{ex}} = 328 \text{ nm}$). The emission spectrum of **P2** demonstrates a broad band having a main peak at 447 nm which was attributed to twisted intramolecular charge transfer (TICT) emission of dansyl in which dimethyl amino and naphthalene sulfonyl groups act as donor and acceptor parts, respectively.⁴⁵ TICT band, also called as Band A, is sensitive to the polarity of the fluorescence medium.⁴⁶ When the fluorescence emission spectra of **P2** were taken in solutions with different polarity (obtained by adding water to ACN solution of **P2**), the emission bands red-shifted to 490 nm and were observed to be more symmetric (Figure 5).

The binding and recognition characteristics of the dansyl end-functional PCL star polymer (**P2**) toward various metal ions

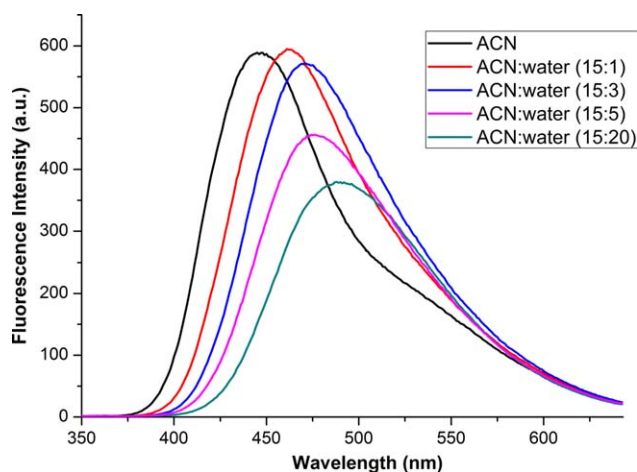


Figure 5. Fluorescence emission spectra of **P2** ($2.05 \times 10^{-5} \text{ M}$) in ACN and ACN : water solvent mixtures. [Color figure can be viewed in the online issue, which is available at wileyonlinelibrary.com.]

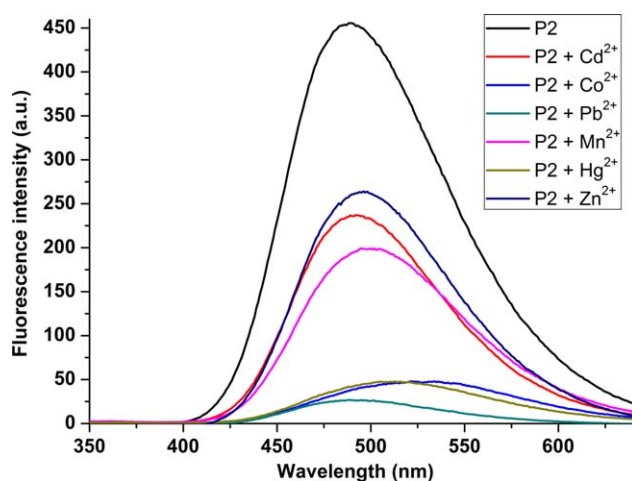


Figure 6. The fluorescence emission spectra of **P2** ($1.34 \times 10^{-5} \text{ M}$) in ACN : water (6 : 4) upon addition of 700 eq. of metal cations. [Color figure can be viewed in the online issue, which is available at wileyonlinelibrary.com.]

were determined via fluorescence spectrophotometric measurements using 1-cm path length cuvettes. Metal ion sensing experiments of **P2** were performed in ACN : water (6 : 4) solvent mixtures at 328 nm excitation wavelength at room temperature and the related fluorescence emission spectra are depicted in Figures 6 and 7. In these spectra, in the absence of metal cations, intramolecular charge transfer (ICT) from the nitrogen atom of the dimethylamino moiety to naphthalene group was effective.¹⁰ Upon titration of **P2** with 700 equivalent of Cd^{2+} , Co^{2+} , Hg^{2+} , Pb^{2+} , Mn^{2+} , and Zn^{2+} cations, ICT emission intensity of dansyl fluorophore was observed to decrease remarkably with concomitant slight red-shifting of band maxima (Figure 6). This phenomenon was attributed to electron transfer from the excited dansyl fluorophore to the proximate metal cations.⁴⁷ Among the studied metal cations, the highest quenching efficiency was observed for Pb^{2+} . The evolution of

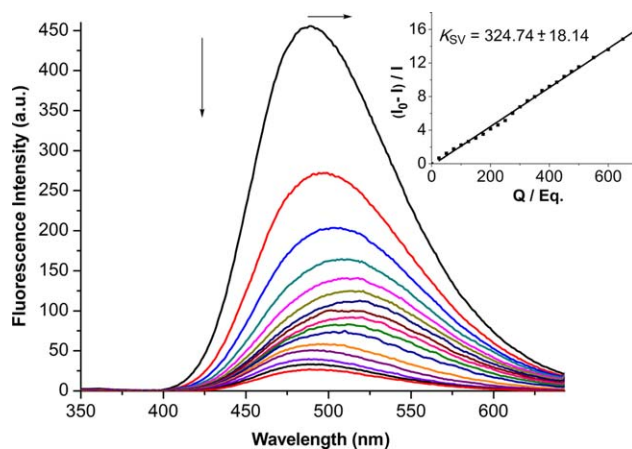


Figure 7. Fluorescence emission spectra of **P2** ($1.34 \times 10^{-5} \text{ M}$) in ACN : water (6 : 4) in the presence of Pb^{2+} cation at 25, 50, 75, 100, 125, 150, 175, 200, 225, 250, 300, 350, 450, 550, and 700 equivalent ratios. [Color figure can be viewed in the online issue, which is available at wileyonlinelibrary.com.]

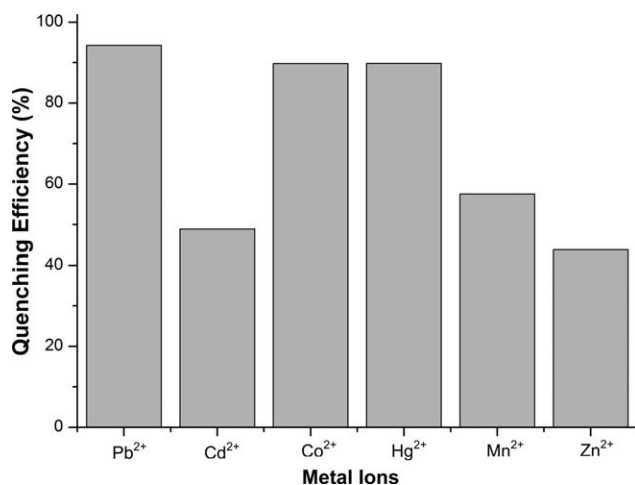


Figure 8. Quenching efficiency ratios for the fluorescent emission intensities of **P2** upon the addition of 700 eq. metal ions.

fluorescence emission spectra of **P2** upon titration with Pb²⁺ cation at different equivalent (Eq.) ratios is depicted in Figure 7. The Stern–Volmer plot in the inset of Figure 7 suggests that the quenching process of **P2** by the addition of Pb²⁺ cations is rather linear with the increasing concentration of the quencher. These results indicate a dynamic (collisional) quenching mechanism in which energy of the excited fluorophore was transferred nonradiatively to the quencher.^{48,49} Besides, calculated Stern–Volmer constant ($K_{SV} = 324.74 M^{-1}$) for **P2** : Pb²⁺ complex is relatively high and points out a strong interaction between dansyl fluorophore and Pb²⁺ cation. Stern–Volmer plots for the interaction of **P2** with other cations deviated from linearity. Thus, K_{SV} for the other cations were calculated from the initial linear parts of the plots. The obtained K_{SV} values for Co²⁺, Hg²⁺, Mn²⁺, Zn²⁺, and Cd²⁺ cations were 212.33, 189.21, 36.24, 20.84, and 20.69, respectively. These values reflect their relative interaction strengths with **P2** and one can conclude that **P2** has selectivity toward Pb²⁺ over the other cations to some extent. Moreover, quenching efficiency ratios (QE) of Pb²⁺, Co²⁺, Hg²⁺, Mn²⁺, Zn²⁺, and Cd²⁺ cations were calculated using the formula: $QE = ((I_0 - I)/I_0) \times 100$. The results are briefly depicted in Figure 8. The highest quenching (94.24%) efficiency was attained in the presence of Pb²⁺ ions. As shown in Figure 8, except for Hg²⁺ and Co²⁺, other background metal ions had small interferences for the fluorogenic determination of Pb²⁺ cation suggesting that **P2** could be employed as a potential Pb²⁺ chemical probe.

CONCLUSION

Hexa-armed PCL star polymer having fluorescent-active dansyl end groups and phosphazene core (**P2**) was prepared via ROP of ϵ -CL and esterification reactions. Data obtained from FTIR and ¹H-NMR spectral analysis confirmed the successful synthesis of the polymers. **P2** gave characteristic UV and fluorescence emission bands for the dansyl fluorophore, indicating the presence of dansyl end-groups. Upon the addition of Pb²⁺, Co²⁺, Hg²⁺, Mn²⁺, Zn²⁺, and Cd²⁺ cations, fluorescence emission of **P2** was considerably quenched due to suppression of TICT process of dansyl unit. The highest quenching efficiency was observed for

Pb²⁺ cation. Besides, Stern–Volmer plot for the interaction of **P2** with Pb²⁺ was rather linear, indicating collisional (dynamic) quenching process. The higher K_{SV} value for Pb²⁺ compared to other metal cations points out the potential of **P2** to be used in the selective fluorogenic determination of Pb²⁺ cation.

ACKNOWLEDGMENTS

The authors gratefully thank the Istanbul Medeniyet University Research Foundation (Grant number FBA-2012-167) for financial support.

REFERENCES

- Métivier, R.; Leray, I.; Valeur, B. *Chem.—Eur. J.* **2004**, *10*, 4480.
- Abebe, F. A.; Eribal, C. S.; Ramakrishna, G.; Sinn, E. *Tetrahedron Lett.* **2011**, *52*, 5554.
- Zhang, L.; Li, Q.; Zhou, J.; Zhang, L. *Macromol. Chem. Phys.* **2012**, *213*, 1612.
- An, F.; Gao, B.; Feng, X. *J. Appl. Polym. Sci.* **2009**, *112*, 2241.
- Buica, G.-O.; Ungureanu, E.-M.; Birzan, L.; Razus, A. C.; Mandoc, L.-R. *J. Electroanal. Chem.* **2013**, *693*, 67.
- Saadeh, H. A.; Shairah, E. A. A.; Charef, N.; Mubarak, M. S. *J. Appl. Polym. Sci.* **2012**, *124*, 2717.
- Kim, I.-B.; Dunkhorst, A.; Gilbert, J.; Bunz, U. H. F. *Macromolecules* **2005**, *38*, 4560.
- Ge, H.; Chen, H.; Huang, S. *J. Appl. Polym. Sci.* **2012**, *125*, 2716.
- Tang, J.; Sun, J.; Xu, J.; Li, W. *J. Appl. Polym. Sci.* **2014**, *131*, 39973.
- Dhir, A.; Bhalla, V.; Kumar, M. *Org. Lett.* **2008**, *10*, 4891.
- Pan, J.; Wang, S.; Zhang, R. *J. Appl. Polym. Sci.* **2006**, *102*, 2372.
- Chen, Y.; Zhu, C.; Yang, Z.; Li, J.; Jiao, Y.; He, W.; Chen, J.; Guo, Z. *Chem. Commun.* **2012**, *48*, 5094.
- Li, D.; Li, H.; Liu, M.; Chen, J.; Ding, J.; Huang, X.; Wu, H. *Macromol. Chem. Phys.* **2014**, *215*, 82.
- Lei, Y.; Ma, F.; Tian, Y.; Niu, Q.; Mi, H.; Nurulla, I.; Shi, W. *J. Appl. Polym. Sci.* **2013**, *129*, 1763.
- Ojida, A.; Takashima, I.; Kohira, T.; Nonaka, H.; Hamachi, I. *J. Am. Chem. Soc.* **2008**, *130*, 12095.
- Güney, O.; Cebeci, F. Ç. *J. Appl. Polym. Sci.* **2010**, *117*, 2373.
- Bu, J.-H.; Zheng, Q.-Y.; Chen, C.-F.; Huang, Z.-T. *Org. Lett.* **2004**, *6*, 3301.
- Liu, Y.; Miao, Q.; Zhang, S.; Huang, X.; Zheng, L.; Cheng, Y. *Macromol. Chem. Phys.* **2008**, *209*, 685.
- Rabindranath, A. R.; Maier, A.; Schäfer, M.; Tieke, B. *Macromol. Chem. Phys.* **2009**, *210*, 659.
- Wen, Q.; Zhu, C.; Liu, L.; Yang, Q.; Wang, S.; Zhu, D. *Macromol. Chem. Phys.* **2012**, *213*, 2486.
- Ciardelli, G.; Saad, B.; Lendlein, A.; Neuenschwander, P.; Suter, U. W. *Macromol. Chem. Phys.* **1997**, *198*, 1481.

22. Miao, Q.; Huang, X.; Cheng, Y.; Liu, Y.; Zong, L.; Cheng, Y. *J. Appl. Polym. Sci.* **2009**, *111*, 3137.
23. Huang, W.; Wu, W. *J. Appl. Polym. Sci.* **2012**, *124*, 2055.
24. Silva, A. J. C.; Silva, J. G., Jr.; Alves, S., Jr.; Tonholo, J.; Ribeiro, A. S. *J. Braz. Chem. Soc.* **2011**, *22*, 1808.
25. Liu, Z.; He, W.; Guo, Z. *Chem. Soc. Rev.* **2013**, *42*, 1568.
26. Horie, K.; Yamada, S.; Machida, S.; Takahashi, S.; Isono, Y.; Kawaguchi, H. *Macromol. Chem. Phys.* **2003**, *204*, 131.
27. González-Benito, J.; Mikeš, F.; Baselga, J.; Lemetyinem, H. *J. Appl. Polym. Sci.* **2002**, *86*, 2992.
28. Zhao, Y.; Zhong, Z. *J. Am. Chem. Soc.* **2006**, *128*, 9988.
29. Miao, R.; Zheng, Q.-Y.; Chen, C.-F.; Huang, Z.-T. *Tetrahedron Lett.* **2004**, *45*, 4959.
30. Qiu, L.; Jiang, P.; He, W.; Tu, C.; Lin, J.; Li, Y.; Gao, X.; Guo, Z. *Inorg. Chim. Acta* **2007**, *360*, 431.
31. Yin, J.; Guan, X.; Wang, D.; Liu, S. *Langmuir* **2009**, *25*, 11367.
32. Gorur, M.; Yilmaz, F.; Kilic, A.; Sahin, Z. M.; Demirci, A. *J. Polym. Sci. Part A: Polym. Chem.* **2011**, *49*, 3193.
33. Ohno, S.; Gao, H.; Cusick, B.; Kowalewski, T.; Matyjaszewski, K. *Macromol. Chem. Phys.* **2009**, *210*, 421.
34. Aydin, M.; Atilla Tasdelen, M.; Uyar, T.; Yagci, Y. *J. Polym. Sci. Part A: Polym. Chem.* **2013**, *51*, 5257.
35. Gorur, M.; Yilmaz, F.; Kilic, A.; Demirci, A.; Ozdemir, Y.; Kosemen, A.; Eren San, S. *J. Polym. Sci. Part A: Polym. Chem.* **2010**, *48*, 3668.
36. Yuan, W.; Huang, X.; Tang, X. *Polym. Bull.* **2005**, *55*, 225.
37. Rele, S. M.; Cui, W.; Wang, L.; Hou, S.; Barr-Zarse, G.; Tatton, D.; Gnanou, Y.; Esko, J. D.; Chaikof, E. L. *J. Am. Chem. Soc.* **2005**, *127*, 10132.
38. Altintas, O.; Hizal, G.; Tunca, U. *Des. Monomers Polym.* **2009**, *12*, 83.
39. Gunay, U. S.; Durmaz, H.; Gungor, E.; Dag, A.; Hizal, G.; Tunca, U. *J. Polym. Sci. Part A: Polym. Chem.* **2012**, *50*, 729.
40. Yuan, W.; Yuan, J.; Zhou, M.; Pan, C. *J. Polym. Sci. Part A: Polym. Chem.* **2008**, *46*, 2788.
41. Gyun Shin, I. L.; Yeon Kim, S.; Moo Lee, Y.; Soo Cho, C.; Yong Kiel, S. *J. Controlled Release* **1998**, *51*, 1.
42. Yuan, W.; Tang, X.; Huang, X.; Zheng, S. *Polymer* **2005**, *46*, 1701.
43. Yuan, W.; Yuan, J.; Zhou, M.; Sui, X. *J. Polym. Sci. Part A: Polym. Chem.* **2006**, *44*, 6575.
44. Flink, S.; van Veggel, F. C. J. M.; Reinhoudt, D. N. *Chem. Commun.* **1999**, 2229.
45. Ding, L.; Fang, Y.; Jiang, L.; Gao, L.; Yin, X. *Thin Solid Films* **2005**, *478*, 318.
46. Ren, B.; Gao, F.; Tong, Z.; Yan, Y. *Chem. Phys. Lett.* **1999**, *307*, 55.
47. Chen, Q.-Y.; Chen, C.-F. *Tetrahedron Lett.* **2005**, *46*, 165.
48. Sahoo, B. K.; Ghosh, K. S.; Dasgupta, S. *Biopolymers* **2009**, *91*, 108.
49. Anzenbacher, P.; Mosca, L.; Palacios, M. A.; Zyryanov, G. V.; Koutnik, P. *Chem.—Eur. J.* **2012**, *18*, 12712.